Synthesis of a Phosphorus/Silicon Hybrid and Its Synergistic Effect with Melamine Polyphosphates on Flame Retardant Polypropylene System

Y. W. Huang, M. L. Song, J. J. Ma, Z. Y. Lu, J. X. Yang, K. Cao

State Key Laboratory Cultivation Base for Nonmetal Composite and Functional Materials & School of Material Science and Technology, Southwest University of Science and Technology, Mianyang 621010, People's Republic of China
Correspondence to: K. Cao (E-mail: caoke@swust.edu.cn)

ABSTRACT: A novel flame retardant (SDPS) containing P—O—Si bands was synthesized by a condensation polymerization of diphenylhydroxysilane and spirocyclic pentaerythritol di(phosphate monochloride). The structure of SDPS was confirmed by Fourier transform infrared spectroscopy (FTIR) and ^{1}H nuclear magnetic resonance (^{1}H NMR). Limiting oxygen index (LOI) test showed that when loading 22.5 wt % SDPS and 7.5 wt % in polypropylene, LOI value markedly increased to 31.4% in comparison with PP/SDPS (30 wt %) and PP/MP (30 wt %) systems. Combusting experiment further proved a synergistic effect of SDPS and melamine polyphosphates (MP) in flame retarding of polypropylene. Thermogravimetric analysis (TGA) and FTIR-TG results revealed that the synergistic effect was attributed to a catalyzed breaking down of P—O—Si bands in the presence of MP, which acted as an acid catalyst, consequently leading to a facilitated char and silica forming process. © 2012 Wiley Periodicals, Inc. J. Appl. Polym. Sci. 129: 316–323, 2013

INTRODUCTION

Polypropylene (PP) is nowadays used widely in many fields, such as automobiles, housing and electronic and electric industry. Unfortunately, its application is greatly limited due to the tindery property.[1] Hence, a large number of advanced flame retardants have been developed in the past few decades. The most promising approaches involve the utilization of phosphorus- and silicon compounds.

Phosphorus-containing compounds are the most common halogen-free flame retardants, which show promising application in variety of polymer matrixes.[2,3] In the condensed phase, thermal decomposition of phosphorus-containing compounds leads to the production of phosphoric acid and pyrophosphoric acid, which can catalyze the formation of carbonized layer. This charring layer will isolate and protect the polymer from the flames. On the other hand, phosphorus-based flame retardants can also volatilize into the gas phase, consequently forming active radicals, such as PO_2, PO, HPO, etc, which act as scavengers of H and OH radicals. Moreover, phosphorus-based flame retardant, as a carbonization agent, can be combined with a blowing agent like nitrogen-containing compounds and an acid source such as polyatomic alcohol to construct intumescent flame retardation (IFR), consequently leading to outstanding flame retarding performance.[4] Although the phosphorus-based flame retardants demonstrated better flame retardancy than many other halogen-free flame retardants,[2,3,5] high loadings are generally needed to achieve UL94-V0 rating in PP.[6–8] In addition, conventional phosphorus-containing additives are hydrophilic and hygroscopic, which displays low compatibility with hydrophobic PP materials. This would lead to the reduction in mechanical strength and the migration of the flame retardants to the surface. On the other hand, silicon-containing flame retardants are considered as one of alternatives of phosphorus-containing flame retardants, in regarding to their environment-friendliness, high heat resistance and anti-dripping property.[9] More importantly, they could migrate to the surface of polymer matrix at high temperature due to their low surface energy, forming a protective silica layer to hamper the penetration of air and heat into polymers.[10–14] However, many studies have revealed that the utilization of only silicon-containing compounds scarcely provide enough flame retardancy.[13–16]

Recently, combining phosphorus and silicon has received much attention.[17–26] Early investigations proved that phosphorus and silicon indeed show some synergy effect in flame retarding. The P—Si synergistic mechanism of flame retardation was described that phosphorus provides a tendency for char formation and

silicon favorably provides an enhancement of the thermal stability of the char, resulting in a high efficiency of char formation. However, satisfied flame retardancy was not always reported in the phosphorus-silicon hybrid systems.[27–29] As described earlier, this could be attributed to the low phosphorus-containing contents and hydrophilic functional groups.[20] Nevertheless, in some cases, highly improved fire resistance was attainable even when the phosphorus content in P—Si hybrid is low.[25] Moreover, the flame retardants combining APP or MP with silicon generally improve the fire resistance of PA and epoxy resin,[17,20,25,30,31] while gives unsatisfactory performance for the flame retarding of PP.[18,27] Hence, it seems that this flame retarding system is more suitable for the polymeric matrix with high thermostability. This should be firstly due to the poor char forming ability of PP. On the other hand, this is because, we suspect, that the decomposition temperatures of both APP/MP and generally used silicon containing compounds are close to that of PA and epoxy resin while is higher than that of PP. Hence, we inclined to believe that other factors, such as the formation thermodynamic and kinetic of silica and char, play identical important roles in inducing synergistic effect. Further, the reaction in hybridized flame retardants and the interaction between flame retardants and polymeric matrix are of particular important to tailor the formation thermodynamic and kinetic behavior. Revealing above relationships will provide important perspectives for the structure design of P—Si hybrid systems. To achieve this target, design and construction of more new P—Si hybrid systems with variety of structures are required.

In contrast to conventional P—Si hybrids, polymeric P—Si hybrids characteristic of P—O—Si linkage has been rarely studied and may present several merits. Their polymeric structure could effectively inhibit the migration of flame retardants in matrix and facilitate the char forming due to its inherent aggregated morphology. More importantly, P—O—Si bands tend to present an acid catalyzed breaking down. Thus, it can be anticipated that when cooperatively using this P—Si hybrid with polyphosphates, such as APP and MP, these two compounds would present synergistic effect, facilitating the formation of silica and charring layer.

In this work, a novel hybrid flame retardant combining phosphorus and silicon, namely SDPS, was synthesized by a condensation polymerization of diphenylhydroxysilane and spirocyclic pentaerythritol di(phosphate monochloride) (SPDPC). This hybrid possesses polymeric structure with phenyl side groups and with P and Si elements in main chain linked by P—O—Si bands. MP was cooperatively used with this hybrid for the flame retardant of PP. The flame retarding performance was evaluated by limiting oxygen index and combusting experiments. Based on TGA, FTIR, TGA-FTIR, and SEM analysis results, the flame retarding mechanism of MP/SDPS was revealed and an interesting viewpoint was proposed which may provide new perspective for the design of flame retardants.

EXPERIMENTAL

Materials

Phosphorus trichloride, pentaerythritol, methylene dichloride, acetonitrile, acetone, and ether were supplied by KeLong Chemical Industry (Chengdu, China). Acetonitrile (purchased from KeLong) was dried over calcium hydride and distilled at reduced pressure before use. Polypropylene was supplied by Jiangsu Huapai New Material Technology. Diphenyl dichlorosilane was provided by Shanghai Gaolang Chemical Industry (Shanghai, China). Melamine phosphate was supplied by Hefei Finecollection Institute of Chemical Industry.

Synthesis of 3,9-Dichloro-2,4,8,10-tetraoxa-3,9-diphosphaspiroundecane-3,9-dioxide (SPDPC)

Pentaerythritol (0.5 mol) and phosphoryl chloride (3 mol) was mixed in a 500-mL flask equipped with a magnetic stirrer, a thermometer, and a circumference condenser. The mixture was heated at 120°C for 24 h under nitrogen. Resultant solution was filtered and the filtered solids were washed by methylene dichloride and acetone sequentially to remove the unreacted phosphorus oxychloride. The products were dried at 50°C *in vacuo* for 12 h, giving a white powder with the yield of 80%.

Synthesis of Dihydroxydiphenylsilane (DPSD)

About 200-mL deionized water was charged into a 250-mL two-necked glass flask equipped with a mechanical stirrer. Then, 40 mL diphenyl dichlorosilane was added dropwise into the deionized water in 1.5 h with rigorous stir. The filtered products were recrystallized from acetone at 55°C and dried overnight in vacuum at 50°C.

Synthesis of Poly(dihydroxydiphenylsilane substituted dihydroxyl phenyl pentaerythritol diphosphonate) (SDPS)

In a 500-mL three-necked glass flask, 40 g SPDPC (0.140 mol), 29 g DPSD (0.134 mol), and 300 mL acetonitrile were sequentially added. The reaction of as-resulted mixture was conducted at 70°C for 1.5 h and then at 85°C until no HCl gas is emitted. Obtained solution was precipitated in methanol and centrifuged. Resulted solids was dissolved in acetone and precipitated in ether. The vigorous solution was centrifuged and the solids were dried in vacuum at 60°C for 12 h.

Preparation of PP/SDPS Composites

SDPS, MP, and polypropylene were dried at 80°C in vacuum for 6 h. The composites were prepared by blending SDPS, MP, and PP in a HAAKE Rheocord 9000 internal mixer at the rotor rate of 60 rpm at 170°C for 5 min. After mixing, the samples were hot-pressed under 10 MPa for 10 min at 120–130°C into sheets of desired thickness.

Characterization

^{1}H NMR was performed on Bruker Avance 400 using DMSO as a solvent and DMSO as an internal standard. Fourier transform infrared (FT-IR) spectrum were recorded by Nicolet FTIR5700 spectrotphotometer using KBr pellets. Thermogravimetric analysis (TGA) was conducted using a SDT Q600 V20.9 thermal analyzer at a heating rate of $10°C\ min^{-1}$ from room temperature to 800°C under nitrogen/oxygen ratio of 1 : 2. The TG was coupled with a Nicolet FTIR5700 spectrotphotometer for TGA-FTIR investigations. A transfer tube with an inner diameter of 1 mm connected the TG and the infrared cell. Scanning electron microscope (SEM) micrographs of char layer were obtained on TM 1000 (Hitachi, Japan). Limiting oxygen index (LOI) values were measured on an HC-2C oxygen index meter (Jiangning,
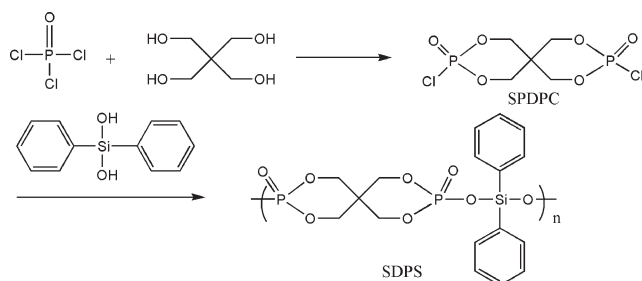
Scheme 1. Synthesis route of SDPS.

China) with sheet dimensions of 100 × 6.5 × 3 mm³ according to the standard oxygen index test ASTM D 2863-97.

RESULTS AND DISCUSSION

Synthesis and Characterization of SDPS

Synthetic route of SPDS is shown in Scheme 1. SPDPC was synthesized according to reported methods.[32,33] The polymerization of SPDPC with diphenylhydroxydisiloxane was facilitated by using triethylamine. The products can precipitate from acetone into methanol and ether, which apparently indicates that the polymerization took place.

FTIR spectrum of SDPS is shown Figure 1. The adsorption band at 1028 cm⁻¹, assignable to P—O—Si stretching, evidences the formation of P—O—Si bands. In addition, characteristic adsorption bands corresponding to P—O—C (998 cm⁻¹), P=O band (1279 cm⁻¹) and phenyl group (1591 cm⁻¹) can be easily seen. In ¹H NMR spectrum of SPDS, the signal of phenyl hydrogen at 7.21–7.45 ppm and CH₂ hydrogen at 3.36 ppm can be found, further supporting the successful synthesis of SDPS. The integration result shows that the ratio of signal intensity of phenyl hydrogen to that of methylene hydrogen is 1 : 0.91. Hence, the DPSD/SPDPC ratio in SDPS can be calculated according to the hydrogen number of SPDPC and DPSD. The calculated ratio is 0.1 : 0.114, indicating that the terminal groups of polymers are SPDPC. This is apparently linked with the excessive feed amount SPDPC relative to that of DPSD. The degree of polymerization, n, can be simply obtained by following equation:

Table I. Compositions and LOI Values of PP/MP, PP/SDPS, and PP/SDPS/MP

Sample	PP (wt %)	SDPS (wt %)	MP (wt %)	SDPS/MP	LOI (%)
PP	100	0	0	–	17.0
PP/SDPS-1	90	10	0	–	19.8
PP/SDPS-2	80	20	0	–	21.3
PP/SDPS-3	70	30	0	–	23.4
PP/MP	70	0	30	–	24.0
PP/SDPS-1/MP	70	7.5	22.5	1 : 3	26.8
PP/SDPS-2/MP	70	15	15	1 : 1	31.2
PP/SDPS-3/MP	70	22.5	7.5	3 : 1	34.0

$$\frac{n+1}{n} = 0.114/0.1$$

So n is ∼7. The molecular weight can be calculated by:

$$(M_{SPDPC} + M_{DPSD} - M_{HCl}) \times 7 + M_{SPDPC} - M_{Cl} + M_{OH}$$

The obtained value is 3486 g mol⁻¹. The P and Si percentages can also be easily calculated, which are 6.2 and 5.6 wt %, respectively.

Flammability of PP Composites

The compositions of PP/MP, PP/SDPS, and PP/SPDS/MP samples studied in this work are summarized in Table I. The flammability of composites was evaluated by limiting oxygen index (LOI) test. As can be seen, when the content of SDPS in PP was increased from 10 to 30 wt %, LOI values were increased to 23.4 %, which was indicative of the absence P/Si synergistic effect in SDPS. This also implies that P/Si synergistic effect is hardly obtained by simply combining phosphorus and silicon elements in one compound. Moreover, the loading of 30 wt % MP in PP led to a LOI value of 24%, which was closed to the value that obtained in PP/30% SDPS. This reveals that MP alone, which is a typical intumescent flame retardant generating porous charring layer, could not provide satisfactory
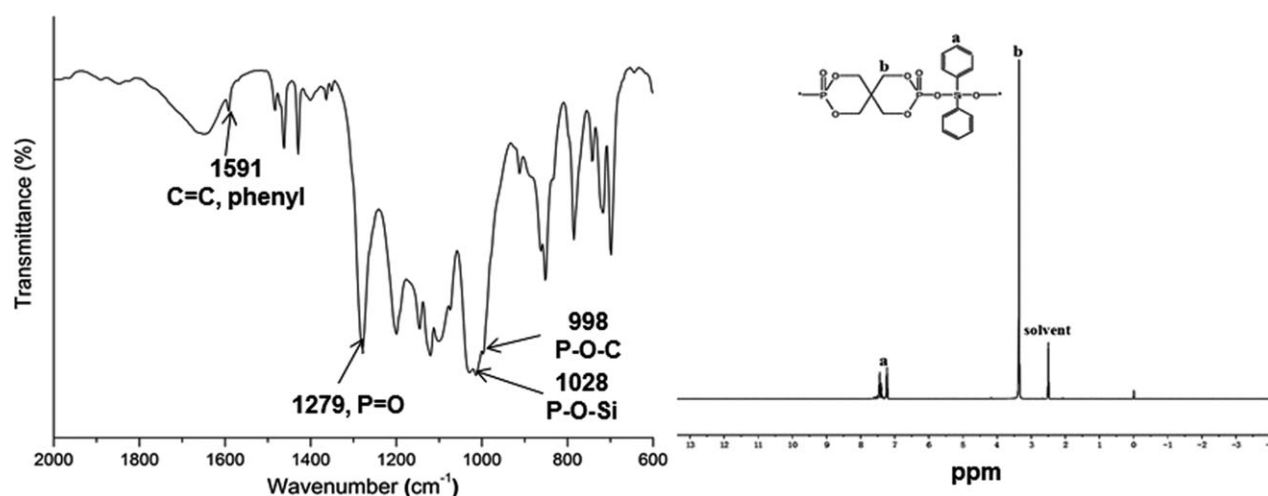

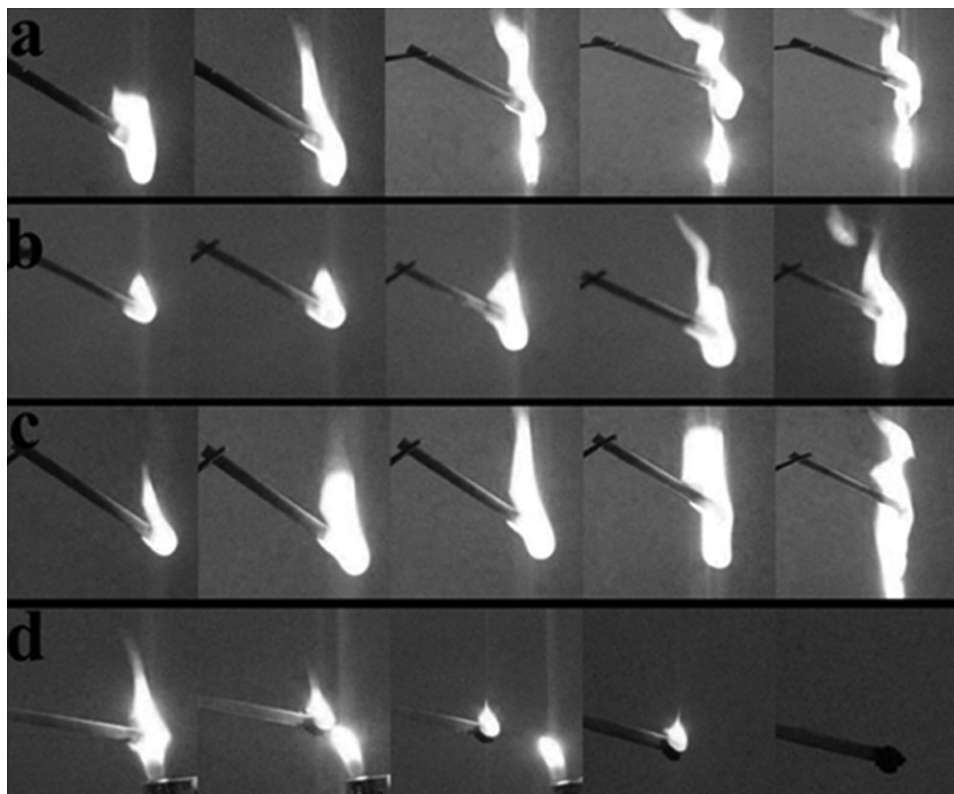**Figure 1.** FTIR spectra (left) and ¹H NMR spectra (right) of SDPS.

Figure 2. Combusting process of (a) PP, (b) PP/SDPS-3, (c) PP/MP, and (d) PP/SDPS/MP-3.

performance. More importantly, this implies that high phosphorus content could not always result in good fire resistance, in particular for polyolefins. When SDPS and MP were cooperatively used, LOI values were pronounced improved, which evidenced a synergistic effect between SDPS and MP. The highest LOI value obtained in this study was 34% when employing 22.5 wt % SDPS and 7.5 wt % MP with the SDPS/MP ratio of 3 : 1. Contrastively, the use of SDPS/MP ratios of 1 : 1 and 1 : 3 only led to a slight increase in LOI value. Apparently, the ratio of intumescent agents to silicon should be an important parameter which was directly correlated to flammability.

The combusting behavior of the samples was shown in Figure 2. It can be clearly seen that pristine PP show a continuous flaming and obvious dripping. Incorporating MP or SPDS alone hardly hampers the flaming, although reduce the dripping. In contrast, the cooperative use of MP and SPDS markedly inhibited flaming. The sample strip show rapid extinguishing within a few seconds. Meanwhile, compact carbonaceous char was likely generated, which may be originated from the formation of silica. To further understand the flame retarding mechanism of SDPS/MP system and the synergistic effect between SDPS and MP, TGA, FTIR and TGA-IR were conducted as following.
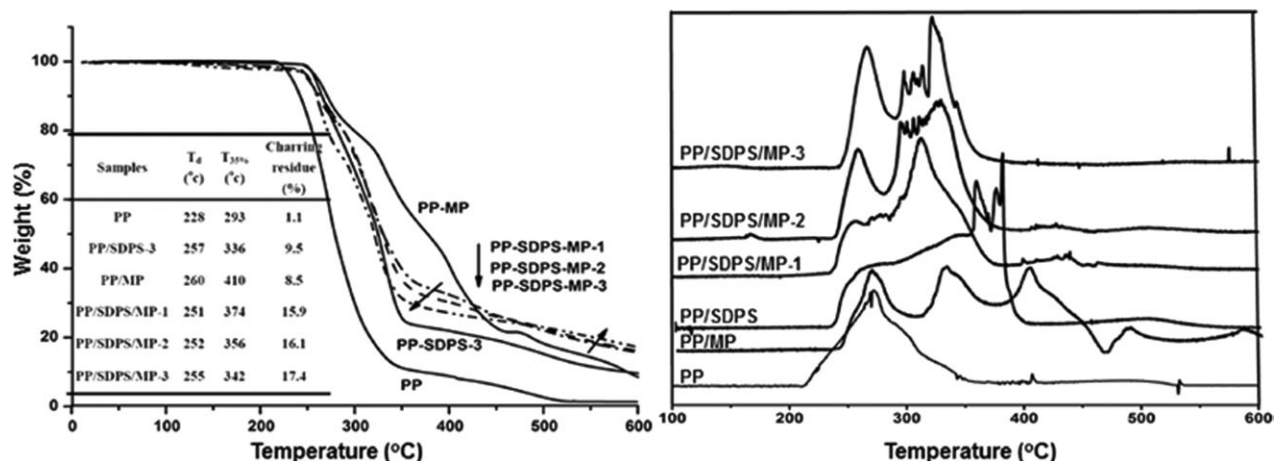

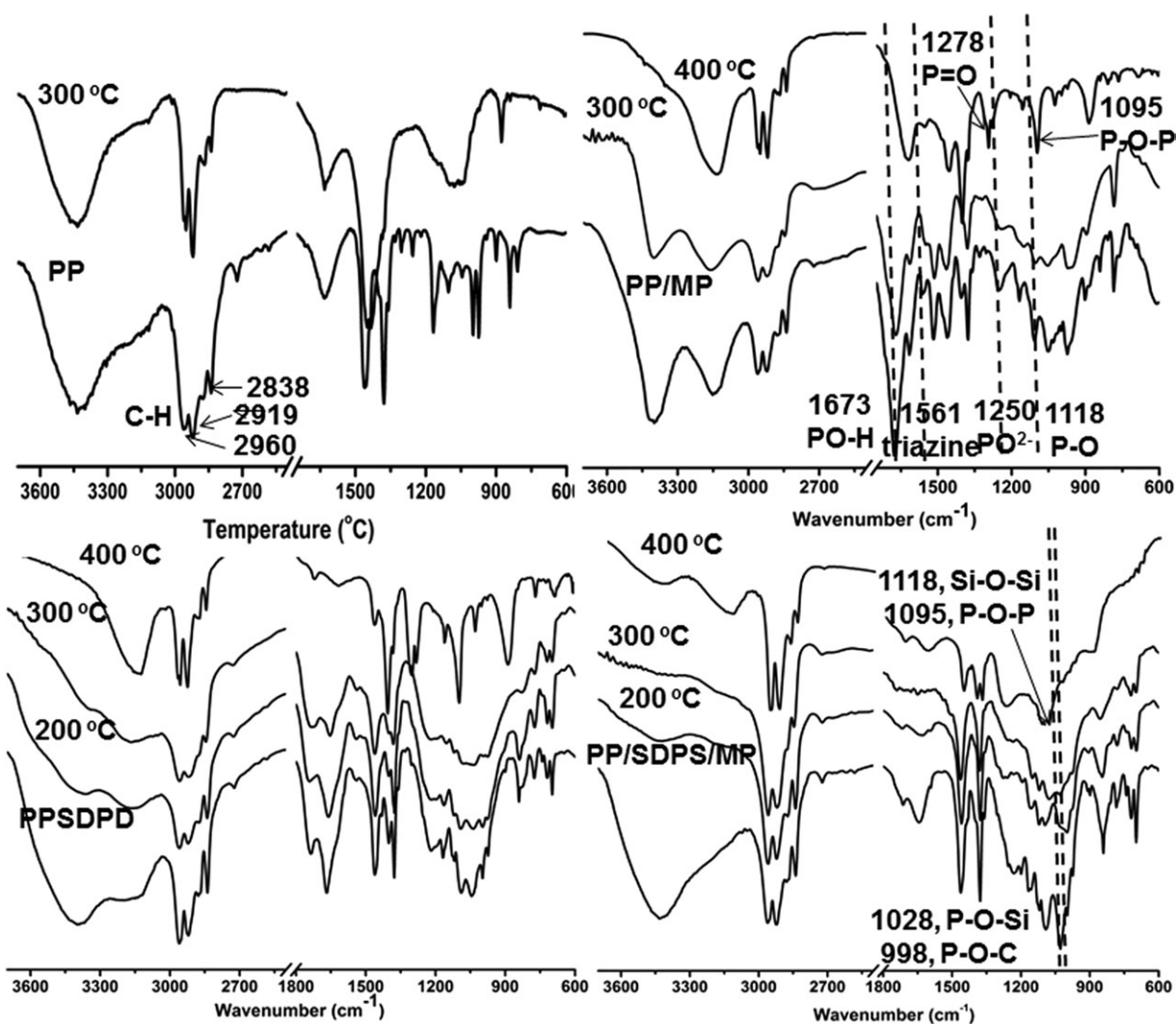**Figure 3.** TG and DTG curves of PP and PP composites.

Figure 4. FTIR spectra of the thermal degradation process of PP/SDPS/MP hybrids: (a) PP; (b) PP/SDPS-; (c) PP/MP; (d) PP/SDPS/MP-3.

Thermogravimetric Analysis of PP and PP Composites

TGA was used to analysis thermal degradation of the polymer composites. Figure 3 presents TGA and DTG curves of PP, PP/MP, and PP/MP/SDPS. The onset decomposition temperature (T_d), 65 wt % weight loss temperature ($T_{65\%}$) and the residue weight ratio are summarized in Figure 3(a). First of all, it can be clearly seen that the loading of SDPS in PP markedly improves the thermal stability of PP and increased charring amount. However, in contrast to PP/MP composite, PP/SPDS composite showed a relatively rapid decomposition and char/silica forming process. Attractively, although it didn't result in a remarkable increase in thermal stability, the cooperative use of SPDS and MP leads to an improvement in charring residue content from ~10 to 16%. Normally, this would result in a reduction in the flammability of polymers. However, as mentioned above, in the several used SDPS/MP ratios, only the use of the ratio of 3 : 1 led to a pronounced increase of LOI. Moreover, with increasing the SDPS/MP ratio from 1 : 3 to 3 : 1, T_d showed a non-negligible decrease while charring residue content showed a slight increase. Hence, we suggest that the high LOI

value for PP/SDPS/MP-3 could not be easily attributed to the charring residue amount, but may be originated from some other factors, such as the thermodynamic and kinetic of silica and char forming process.

DTG analysis provided additional detailed information of decomposition process. First, it can be seen that PP displays two-step decomposition at the range of 243–283°C and 283–363°C, respectively. In contrast, PP/SDPS and PP/MP shows more complicate decomposition, including an additional decomposition at relatively high temperature. This indicates that the flame retarding effect of SDPS and MP may occur after the decomposition of PP, thus resulting in limited flame retarding performance. Moreover, it can be found that the decomposition of PP/SDPS and PP/MP showed several differences. From the DTG curve of PP/SDPS, a facilitated decomposition was observable while this was absence in the DTG of PP/MP. Besides, the decomposition temperature of PP/SDPS was also lower than that of PP/MP. All of them indicate that SDPS enable better char forming relative to MP.
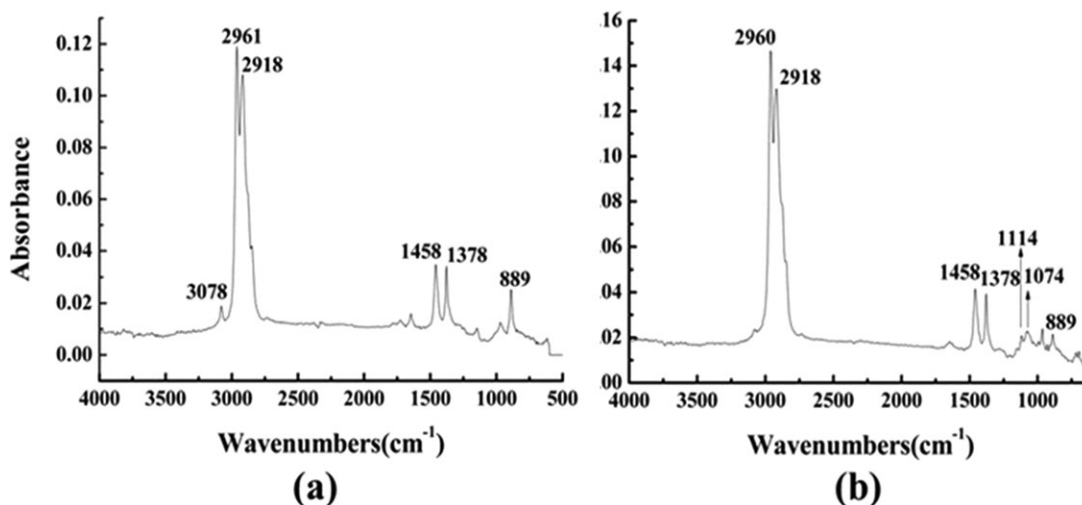
Figure 5. TG-FTIR spectra of (a) PP and (b) PP/SDPS/MP-3.

The cooperative use of SDPS and MP in PP led to a completely different decomposing process in contrast to the use of SDPS or PP alone. Most significant difference which should be noted is that the decomposition peaks of SDPS and MP were invisible in DTG of PP/SDPS/MP and T_{max} of PP/SDPS/MP composites were apparently lower relative to that of PP/SDPS and PP/MP. All of them suggest a facilitated decomposition. Furthermore, from the comparison of DTG curves among PP-SDPS-MP-1, PP-SDPS-MP-2, and PP-SDPS-MP-3, it can be found when increasing SDPS/MP ratio, the area of first peak reflecting the decomposition degree in the first stage (around 250–300°C) was remarkably increased, which further evidences the existence of the facilitated decomposition. We suspect that portions of silica even chars were generated at this stage, which was significantly beneficial to improve the flame retarding effect of charring and silica layers. Overall, TGA and DTG results reveal that the synergistic effect between SDPS and MP resulted in an improvement in char residue content and facilitated char/silica forming process, consequently leading to highly enhanced fire resistance.

Structure Evolution of PP and PP Composites

The synergistic effect between SDPS and MP should be correlated with an interaction between SDPS and MP. To further understand this interaction in depth, FTIR analysis was used (Figure 4) to reveal the structure evolution in the thermal degradation process of PP and PP composites. The samples used for FTIR measurements were fabricated by heating the polymers/KBr composite pellets at 200, 300, and 400°C, respectively, for 10 min. From FTIR spectrum of PP [Figure 4(a)], it can be clearly seen that the intensity of C—H characteristic adsorption bands at 2960, 2919, and 2838 cm^{-1} showed a considerable reduction at 200°C, indicating that the decomposition of PP took place. Figure 4(b) presents FTIR spectra of original PP/MP and PP/MP under heating at 300 and 400°C. In comparison with original PP/MP, FTIR spectrum of PP/MP at 300°C only showed a subtle change, indicating the absence of the decomposition of MP. Contrastively, FTIR spectrum of PP/MP at 400°C showed a pronounced change in characteristic adsorption bands

of MP. The absorption bands at 3413 cm^{-1}, which was attributed to stretching vibration of NH$_2$, almost disappear.[34] Meanwhile, the intensity of absorption band at 1561 cm^{-1} assignable to triazine ring drastically decreases.[35] All of them evidence that the degradation of melamine takes place at 400°C. Moreover, several characteristic adsorption bands of polyphosphates and pyrophosphates at 1095 cm^{-1} (P—O—P) and 1278 cm^{-1} (P=O) appear, accompanied with the disappearance of the characteristic adsorption bands at 1673, 1250, and 1118 cm^{-1} corresponding to PO—H, PO^{2-}, and related P=O bands of melamine polyphosphates. Hence, it could be confirmed that the decomposition of PP-MP at 373–463°C shown in DTG is attributed to the dehydration and deamination of MP. This temperature is obviously higher than the decomposition temperature of PP.

In FTIR spectrum of PP/SDPS composite, a series of adsorption bands at the range of 1000–1100 cm^{-1} can also be seen, which is attributed to P—O—Si and P—O—C stretching as described above. In consistent with PP/MP, PP/SDPS does not decompose at the temperature lower than 300°. Thus, the char forming process catalyzed by SDPS is also later than the decomposition of PP, which is unfavorable for enhancing fire resistance. At 400°C, FTIR spectrum of PP/SDPS shows several remarkable changes, evidencing the decomposition of SDPS. To our surprise, this spectrum was similar with that of PP/MP at 400°C, which supports the formation of only polyphosphates. The characteristic adsorption bands of Si—O—Si at 1100–1200 cm^{-1} were absence. This could be explained by that the silicon containing compounds arising from the decomposition of SDPS may vaporize at high temperature without generating silica. After all, the absence of silica layer should be responsible for the absence of synergistic effect and the unsatisfied flame retarding performance for PP/SDPS.

FTIR spectrum of original PP/SDPS/MP appears to integrate the characteristic adsorption bands of PP/SDPS and PP/MP, including P—O—Si, P—O—C, triazine, and amine groups. However, the decomposition of PP/SDPS/MP was completely different with PP/SDPS or PP/MP. Of particular interest was

that the adsorption band of P—O—Si stretching at 1028 cm^{-1} and P—O—C at 998 cm^{-1} of SDPS almost disappeared at low temperature (200 and 300°C), respectively, which was not observed in the case of PP/SDPS. Correspondingly, apart from the adsorption band of P—O—P at 1095 cm^{-1}, an adsorption band at 1118 cm^{-1}, assignable to Si(Ph)$_2$—O—Si(Ph)$_2$ bands, was observed in FTIR spectrum of PP/SDPS/MP at 400°C. This adsorption band was also absence in corresponding FTIR spectrum of PP/SDPS and PP/MP. All of these results prove that when combined with MP, SDPS exhibits relatively rapid and low temperature decomposition, which shows good consistence with the results of TGA and DTG. Such rapid and low temperature decomposition may be caused by phosphate catalyzed reaction of SDPS. Thus, the synergistic effect in our case not only lies in the well-established P—Si synergistic effect as described in earlier reports, but also lies in the catalyzed decomposition of P—O—Si bands and facilitated char and silica forming by polyphosphates.

TG-FTIR Analysis of PP, PP/SDPS/MP-3

TG-FTIR was used to analyze the gas products during the thermal degradation. Spectra of gas phase in the thermal degradation of PP and PP/SDPS/MP-3 were shown in Figure 5. The evolved gas analysis for both PP and PP/SDPS/MP-3 exhibited characteristic bands of hydrocarbons (2961 cm^{-1}) and olefinic compounds (3078 and 889 cm^{-1}). However, for PP/SDPS/MP, several characteristic adsorption bands of phosphates can be found, such as the band at 1074 and 930 cm^{-1} (P—O—C) and 1114 cm^{-1}(—P—O—P—). Thus, the P containing compounds possibly act in the gas phase.[18,22] Moreover, ammonia was not detected in the gas liberation peak, which gave complementary evidence of chemical interactions between MP and SDPS, enabling N element kept in condensed phase.

CONCLUSION

A novel flame retardant (SDPS) with P—O—Si bands was synthesized by condensation polymerization of diphenylhydroxysilane and spirocyclic pentaerythritol di(phosphate monochloride). Although PP/SDPS didn't show acceptable fire resistance, simultaneously incorporating SDPS and MP endow PP with highly enhanced flame retardancy, proving the existence of synergistic effect. In particular, when utilizing 22.5 wt % SDPS and 7.5 wt % MP, the LOI value reached up to 34%. Combusting experiments also evidence an advantageous extinguishing property of PP/SDPS/MP system, which is attributed to the formation of visible compact charring layer on PP. Degradation, char residue and gas analysis by TGA, TG-FTIR and FTIR further reveals that the synergistic effect was arising from the catalyzed breaking down of P—O—Si bands in SDPS by MP. As a consequence, the facilitated degradation of SDPS led to a reduction in the formation temperature of silica and charring layer, which shows positive effect in improving fire resistance of PP. This, we think, may present significance in the future designation of P—Si hybridized flame retardants. Nevertheless, more studies in depth are still required to support this viewpoint, which will be also a continuous research target of our group.

REFERENCES

1. Zhang, S.; Horrocks, A. R. *Prog. Polym. Sci.* **2003**, *28*, 1517.

2. Laoutid, F.; Bonnaud, L.; Alexandre, M. *Mater. Sci. Eng. R* **2009**, *63*, 100.

3. Lu, S. Y.; Hamerton, I. *Prog. Polym. Sci.* **2002**, *27*, 1661.

4. Vuillequez, A.; Brun, M. L.; Ion, R. M.; Youssef, B. *Macromol. Symp.* **2010**, *290*, 146.

5. Braun, U.; Schartel, B.; Fichera, M. A.; Jager, C. *Polym. Degrad. Stab.* **2007**, *92*, 528.

6. Liu, M.; Liu. Y.; Wang. Q. *Macro. Mater. Eng.* **2007**, *292*, 206.

7. Qiao, Z. H.; Tai, Q. L.; Song, L.; Hu, Y.; Lv, P.; Jie, G. X.; Huang, W.; Fu, Y.; Zhang, D. P. *Polym. Adv. Technol.* **2011**, *22*, 2602.

8. Li, B.; Xu, M. *Polym. Degrad. Stab.* **2006**, *91*, 1380.

9. Hamdani, S.; Longuet, C.; Perrin, D.; Lopez-cuesta, J. M.; Ganachaud, F. *Polym. Degrad. Stab.* **2009**, *94*, 465.

10. Kashiwagi, Y.; Gilman, J. W. In Fire Retardancy of Polymeric Materials, Marcel Dekker Inc., New York; Grand, A. F., Wilkie, C. A., Eds.; **2000**, *10*, 353.

11. Zhong, H. F.; Wei, P.; Jiang, P. K.; Wu, D.; Wang, G. L. *J. Polym. Sci. Part B: Polym. Phys.* **2007**, *45*, 1542.

12. Li, Q.; Jiang, P. K.; Wei, P. *Macro. Mater. Eng.* **2005**, *290*, 912.

13. Masatoshi, L.; Serizawa, S. *Polym. Adv. Technol.* **1998**, *9*, 593.

14. Ravadits, I.; Toth, A.; Marosi, G.; Marton, A. *Polym. Degrad. Stab.* **2001**, *74*, 419.

15. Zhang, S.; Horrocks, A. R. *Prog. Polym. Sci.* **2003**, *28*, 1517.

16. Li, Q.; Zhong, H. F.; Wei, P.; Jiang, P. K. *J. Appl. Polym. Sci.* **2005**, *98*, 2487.

17. Hsiue, G. H.; Liu, Y. L.; Tsiao, J. *J. Appl. Polym. Sci.* **2000**, *78*, 1.

18. Li, Q.; Jiang, P. K.; Su, Z. P.; Wei, P.; Wang, G. L.; Tang, X. Z. *J. Appl. Polym. Sci.* **2005**, *96*, 854.

19. Wang, X.; Hu, Y.; Song, L.; Xing, W. Y.; Lu, H. D. *J. Polym. Sci. Part B: Polym. Phys.* **2010**, *48*, 693.

20. Chen, J.; Liu, S. M.; Zhao, J. Q. *Polym. Degrad. Stab.* **2011**, *96*, 1508.

21. Chen, X. L.; Jiao, C. M. *Fire Safety J.* **2009**, *44*, 1010.

22. Wang, C.; Wei, P.; Qian, Y.; Liu, J. P. *Polym. Adv. Technol.* **2011**, *22*, 1108.

23. Liu, Y.; Wang, D. Y.; Wang, J. S.; Song, Y. P.; Wang, Y. Z. *Polym. Adv. Technol.* **2008**, *19*, 1566.

24. Zhang, L. L.; Liu, A. H.; Zeng, X. R. *J. Appl. Polym. Sci.* **2009**, *111*, 168.

25. Sponton, M.; Mercado, L. A.; Ronda, J. C.; Galia, M.; Cadiz, V. *Polym. Degrad. Stab.* **2008**, *93*, 2025.

26. Sponton, M.; Ronda, J. C.; Galia, M.; Cadiz, V. *Polym. Degrad. Stab.* **2009**, *94*, 145.

27. Li, Q.; Jiang, P. K.; Wei, P. *Polym. Eng. Sci.* **2006**, *46*, 344.

28. Gao, M.; Wu, W. H.; Xu, Z. Q. *J. Appl. Polym. Sci.* **2012**, *127*, 1842.

29. Liu, Y. L.; Wu, C. S.; Chiu, Y. S.; Ho, W. H. *J. Polym. Sci. Part A: Polym. Chem.* **2003**, *41*, 2354.

30. Khurana, P.; Narula, A. K. Choudhary, V. *J. Appl. Polym. Sci.* **2003**, *90*, 1739.

31. Hsiue, G. H.; Liu, Y. L.; Liao, H. H. *J. Polym. Sci. Part A: Polym. Chem.* **2001**, *39*, 986.

32. Xu, H. J.; Jin, F. L.; Park, S. J. *Bull. Korean Chem. Soc.* **2009**, *30*, 2643.

33. Ma, H. Y.; Tong, L. F.; Xu, Z. B.; Fang, Z. P.; Jin, Y. M.; Lu, F. Z. *Polym. Degrad. Stab.* **2007**, *92*, 720.

34. Wang, Z. Z.; Lv, P.; Hu, Y.; Hu, K. L. *J. Anal. Appl. Pyrol.* **2009**, *86*, 207.

35. Zhou, S.; Song, L.; Wang, Z. Z.; Hu, Y.; Xing, W. Y. *Polym. Degrad. Stab.* **2008**, *93*, 1799.